Mainshock-strongest aftershock relation in Northeastern Italy and Western Slovenia

Stefania Gentili[1] and Rita Di Giovambattista[2]

[1]Istituto Nazionale di Oceanografia e di Geofisica Sperimentale
[2]INGV

November 22, 2022

Abstract

In this study, we have applied to northeastern Italy and western Slovenia medium-low seismicity an algorithm for strong aftershock forecasting we originally developed for medium-high seismicity in Italy (Gentili and Di Giovambattista, 2017). This study is possible thanks to the OGS bulletins, an accurate local catalogue, characterized by low completeness magnitude, that has been compiled by the National Institute of Oceanography and Experimental Geophysics, Centre of Seismological Research, since 1977. The method is based on a pattern recognition approach which uses statistical features based on the number of the early aftershocks and on the spatio-temporal evolution of the radiated energy in the first hours/days after the mainshock. The analysis was performed on different time-spans after the mainshock to simulate the increase of information available as time passes during the seismic clusters. Following the approach of Gentili and Giovambattista (2017), we used an operational definition of clusters that defines "mainshock" as the first shock of the cluster over a given threshold. We have adopted this criterion in order to be able to apply the procedure immediately after the occurrence of a shock without waiting to verify if a stronger earthquake followed. If the difference in magnitude between the "mainshock" and the strongest aftershock is lower than 1 the clusters are classified as "Type A", otherwise as "Type B",. The Type A and B clusters' distribution is analyzed also considering a draft subdivision of the region into two sub-regions characterized by different complexity of the clusters (Peresan and Gentili, 2018) Vp/Vs (Bressan et al., 2012) and attenuation characteristcs (Gentili and Gentile, 2015).

AGU100 FALL MEETING

Mainshock-strongest aftershock relation in Northeastern Italy and Western Slovenia

S. Gentili[1] R. Di Giovambattista[2]

[1] Istituto Nazionale di Oceanografia e di Geofisica Sperimentale – Centro Ricerche Sismologiche, Udine, Italy.
[2] Istituto Nazionale di Geofisica e Vulcanologia – Sezione di Roma, Roma, Italy.

AGU100 FALL MEETING

ABSTRACT NUMBER: S43F-0664

1. ABSTRACT

- We investigated the occurrence of large aftershocks following the most significant earthquakes that occurred in **North-eastern Italy** and **Western Slovenia**.
- Clusters are defined as "**type A**" if, given a main shock of magnitude Mm, the **subsequent strongest earthquake** in the cluster has **magnitude Ma≥Mm-1**; of type B otherwise.
- We used an improved version of a pattern recognition method developed by **Gentili and Di Giovambattista 2017** for medium-high seismicity in Italy.
- In particular, we investigated the **radiated energy** and the **the spatio-temporal evolution of the aftershocks** occurring within a few days and the probability to have a strong earthquake depending on the time elapsed after the mainshock.
- In order to characterize the feature depending on the cluster type, we used **decision trees** as classifiers on single feature separately. The **performances** of the classification are tested by **leave-one-out method**.
- The **analysis** was performed on **different time-spans** after the mainshock to simulate the increase of information available as time passes during the seismic clusters.
- The method has been **successfully applied** to the **1976 Friuli cluster**, in which a swarm of large earthquakes happened 4 mounths after the first mainshock and on two small cluster this year in the same are

DATABASE

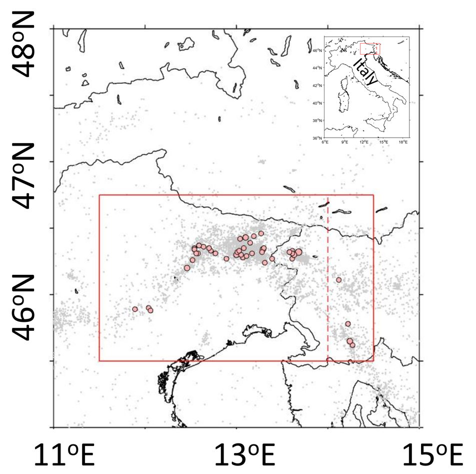

The database we adopted was **OGS Bulletins:** an accurate local catalogue (1977-2018). Mc=2 till 1993 and 1.5 from 1994 (Peresan and Gentili, 2018)

http://www.crs.inogs.it/bollettino/RSFVG/RSFVG.en.html

Fig. 1: Selected area (before and after 2008) and clusters' epicenters (42 clusters)

- The area of sufficient completeness is detected based on the **ratio R** (R>0.8) between the **number of ISC earthquakes that have an equivalent** in OGS catalogue and the **total number** of earthquakes in ISC catalogue (Kossobokov et al. 1999, Peresan and Gentili, 2018).
- **From 2008**, the area could be **extended 0.5 degrees eastward** thanks to the collaboration with ARSO (Environmental Agency of the Republic of Slovenia)

3. CLUSTER IDENTIFICATION

- Clusters were selected by a **windowing algorithm** for the radius ($\boldsymbol{\rho}$) and its duration ($\boldsymbol{\tau}$) identification. In this work the "**mainshock**" is the first event with M≥3.7 in a cluster and "**aftershocks**" are the following events. **42 clusters were detected.**

$$\rho = 10^{0.41M_m - 1} + 2$$
$$\tau = 10^{0.33M_m + 0.42}$$

Gentili and Bressan (2008) + 2 km

- If after the "mainshock" **another event with magnitude ≥ Mm-1 occurs**, the cluster is labeled as being of type "**A**"; **otherwise** it is considered of type "**B**" (Vorobieva 1999).

Fig. 3: Percentage (Perc) of clusters that have had the strongest aftershock. Red=A, Blue=B, black=all.

4. RESULTS: CLUSTERS' CHARACTERISTICS

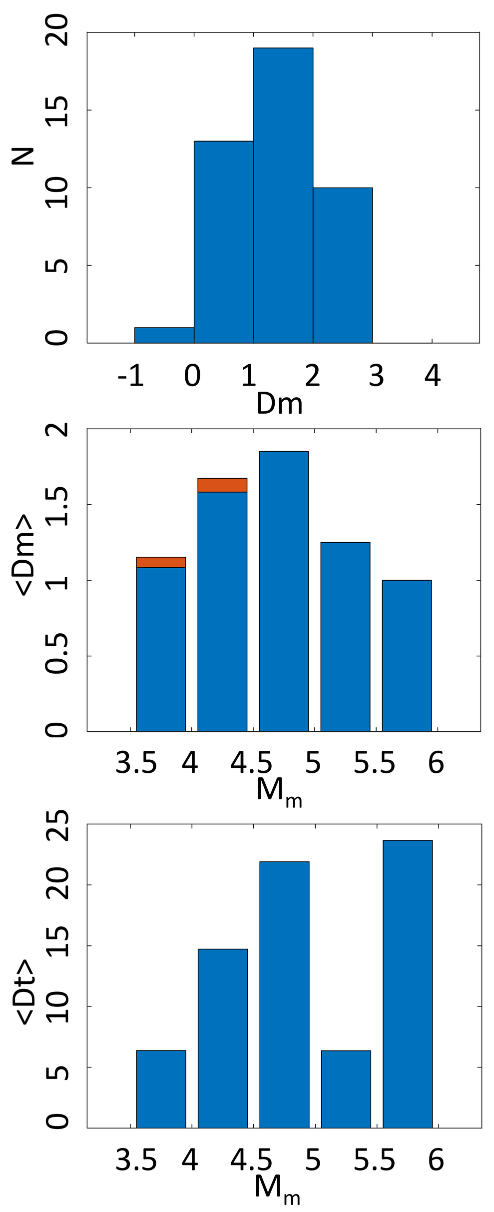

Mean Dm 1.3-1.4 in good agreement with Båth law (Båth, 1965).

For Mm>5 Dm decreases (orange: uncertainty when Ma<Mc).

Dt generally increases with Mm

Fig. 2: Clusters' characteristics: Dm =Mm–Ma; Dt =ta-tm ([Days]); <.> mean of .; a=strongest aftershock

Hp: larger earthquakes activate more complex tectonic structures => the probability to have a subsequent strong event and a longer interval between the mainshock and the strong event is higher.

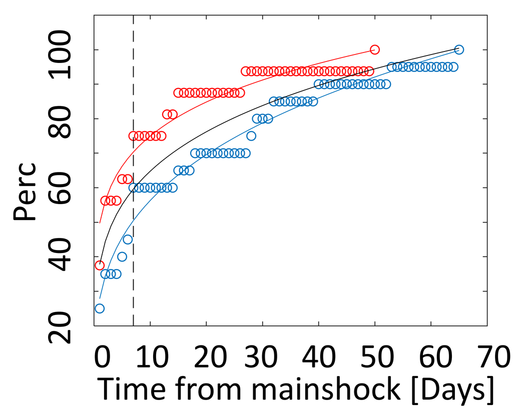

Perc=λT^γ Fitting law

	γ	λ
All data	0.234±0.003	37.8±0.3
A data	0.178±0.005	49.7±0.7
B data	0.306±0.004	27.9±0.6

5. PATTERN RECOGNITION APPROACH

- **NESTORE – (NExt STrOng Related Earthquake)** is a software package for A clusters forecasting based on **pattern recognition** approach. It analyses the seismic data at increasing time intervals T after the mainshock.
- Tested features:
  - **N, N2**=number of aftershocks (with magnitude Mm-2 and Mm-1, respectively)
  - **S**=total equivalent source area
  - **Q**=cumulative radiated energy
  - **Vm**=variation of magnitude from event to event
  - **Vmed**=variation of average magnitude from day to day
  - **Vn**=variation of the number of aftershocks from day to day
  - **Z**=linear concentration of aftershock
  - **SLcum, SLcum2** =deviation of S from the long term trend (SLcum2 with sliding window)
  - **Qlcum, QLcum2**=deviation of Q from the long term trend (QLcum2 with sliding window)
- Accordingly with Gentili and Di Giovambattista (2017), **each feature** has been evaluated by a pattern recognition approach using an **independent decision tree** (Jang et al., 1997).
- A **one-node decision tree** is trained: the algorithm identifies for each feature f a threshold Th so that if **f≥Th** the cluster is identified as **A, otherwise B**.

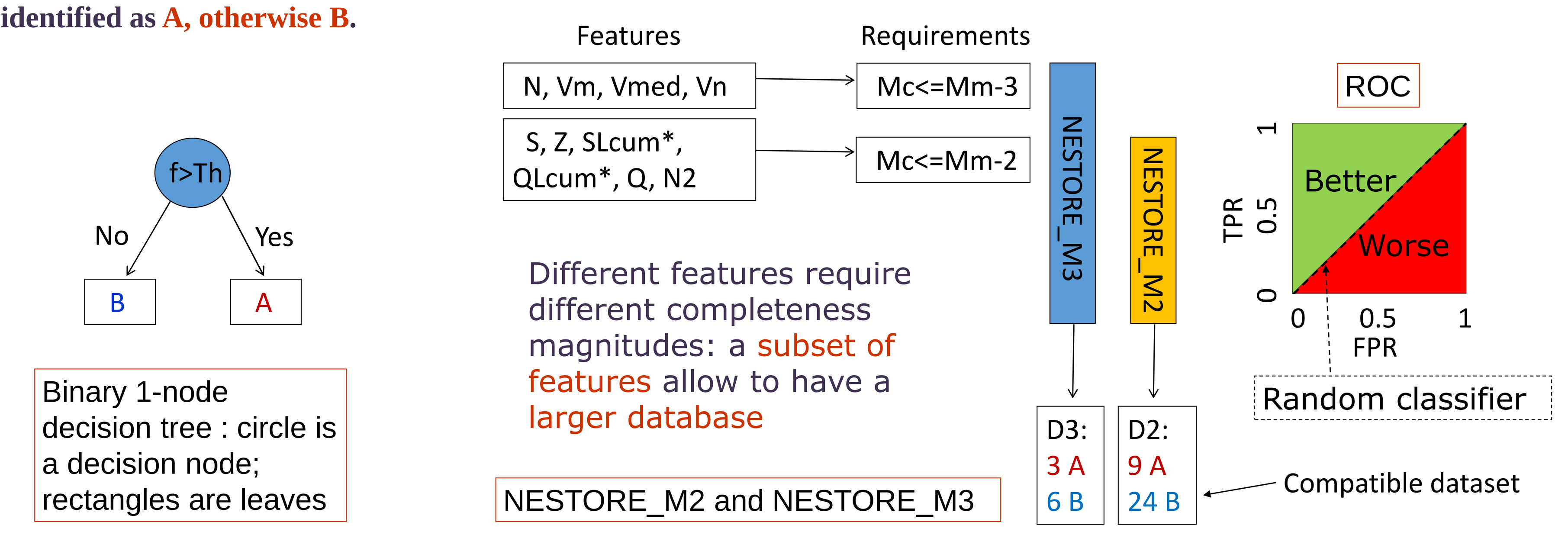

- Using **Mc<=Mm-3** the number of clusters that can be analyzed is **low** => we developed **NESTORE_M2**
- In order to compare precursors performances we selected 6 different time periods (in days: **[0, 0.25] [0,0.5] [0,0.75] [0,1], [0, 2], [0, 3]**) and for each time period we calculated the values of all the tested precursors.
- We checked the performances by the **LeaveOneOut (or LOO)** method: each **learning** set is created by taking **all the samples except one**, the **test** set being **the sample left out**. The procedure is **repeated for all the samples**
- The test allowed to obtain the **confusion matrix** and derived information like **ROC diagrams** (A = p; B = n).

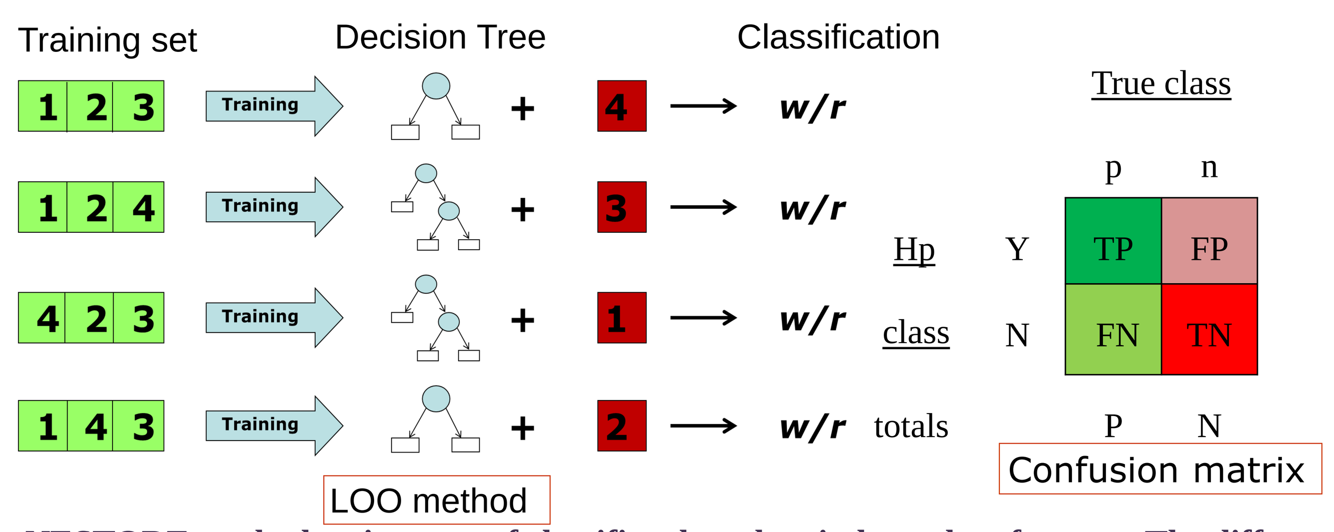

$$Recall = TPR = \frac{TP}{P}$$
$$Precision = \frac{TP}{Y}$$
$$Accuracy = \frac{TP + TN}{P + N}$$
$$FPR = \frac{FP}{N}$$
$$Informedness = TPR - FPR$$

- NESTORE method trains a set of classifiers based on independent features. The different classification results need to be combined in a unique classification "Probability of Class A". We used a **Bayesian approach** (Bailer-Jones et al. 2011):

$$P(A|D_1 \dots D_N) = \frac{[N(B)]^{N-1} \prod_{n=1}^{N} p_n}{[N(B)]^{N-1} \prod_{n=1}^{N} p_n + [N(A)]^{N-1} \prod_{n=1}^{N} (1 - p_n)}$$

p_n=P(A|Dn) is the probability to have A cluster given a value Dn of the n feature, N(A), N(B): number of A, B, N: number of classes.

6. RESULTS: PATTERN RECOGNITION; SINGLE FEATURES

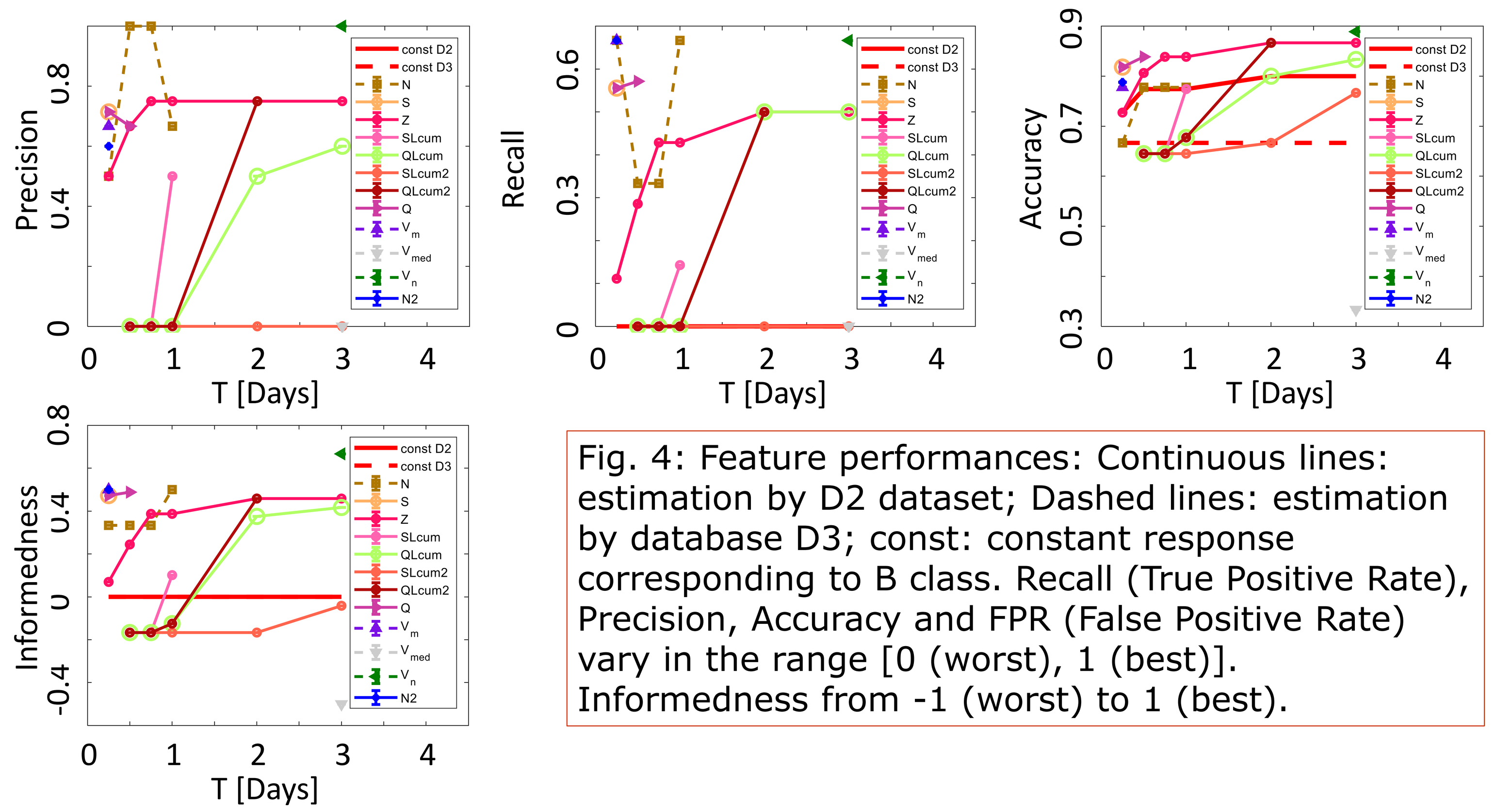

Fig. 4: Feature performances: Continuous lines: estimation by D2 dataset; Dashed lines: estimation by database D3; const: constant response corresponding to B class. Recall (True Positive Rate), Precision, Accuracy and FPR (False Positive Rate) vary in the range [0 (worst), 1 (best)]. Informedness from -1 (worst) to 1 (best).

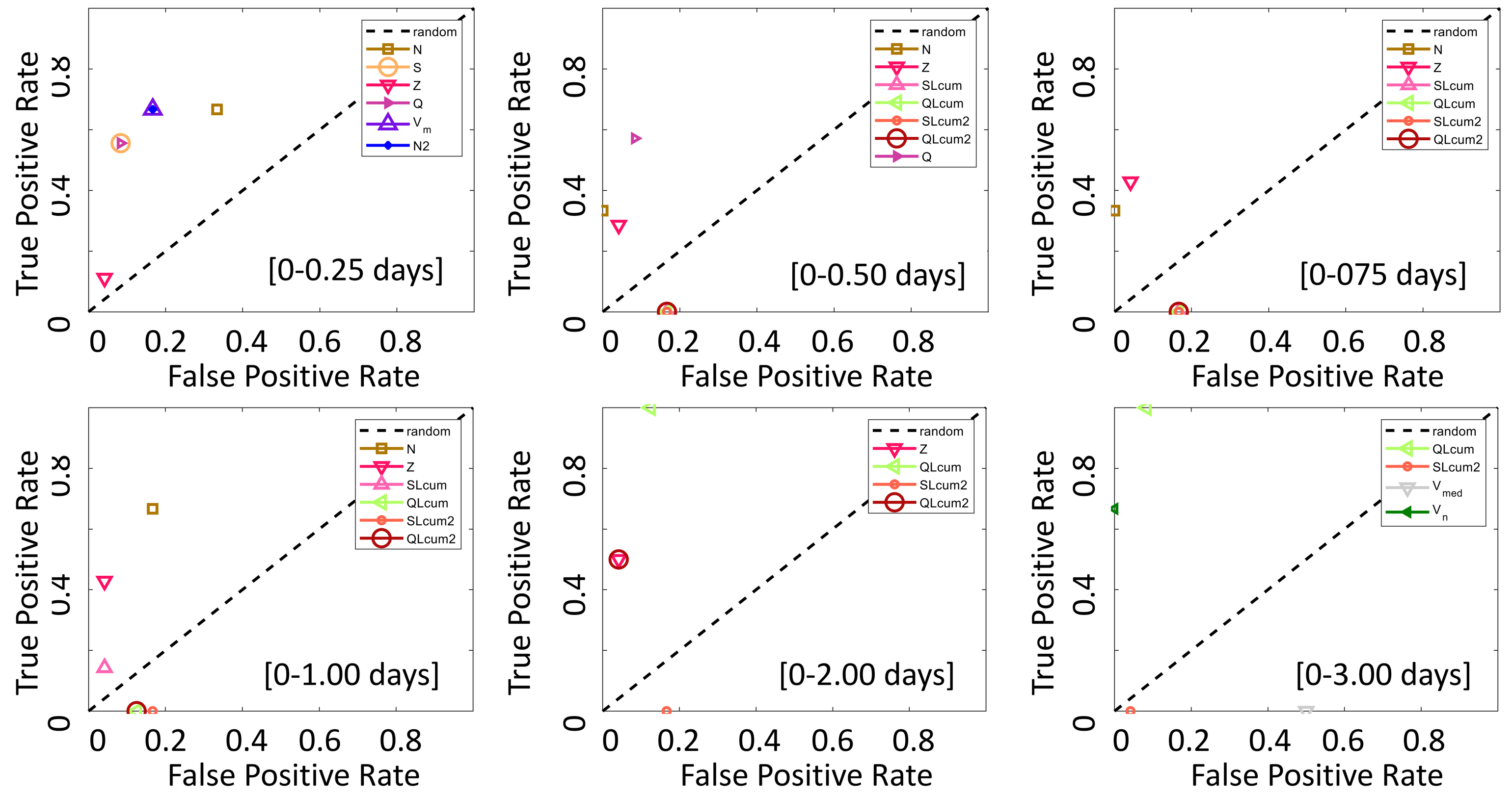

Fig. 5: Receiver Operating Characteristics (ROC) graph (Swets et al., 2000). It depicts the trade-off between benefits (true positives) and costs (false positives)

7. RESULTS: PROB(A) FORECASTING ON INDEPENDENT DATA

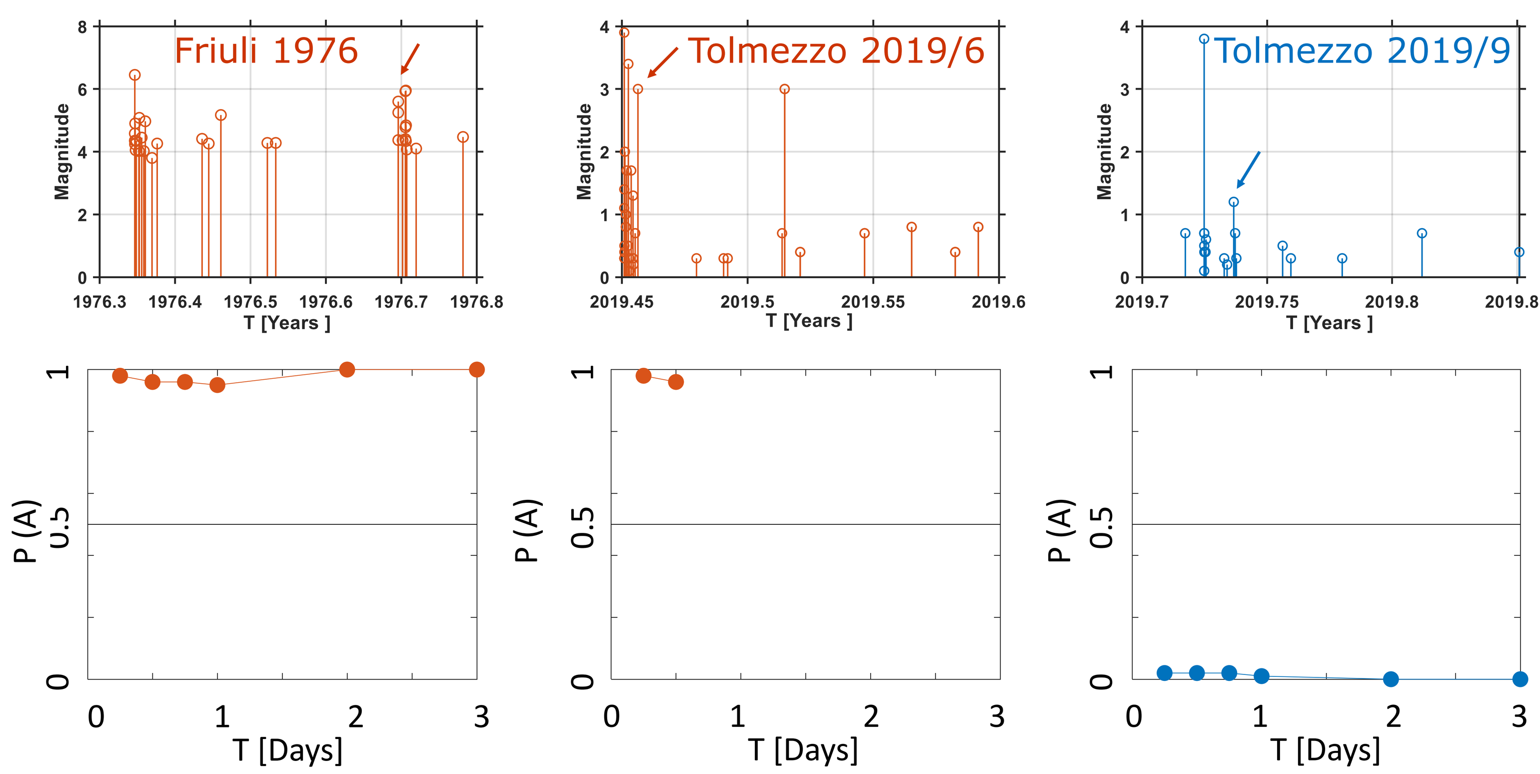

Fig. 6: NESTORE_M2 successfully estimates A probability P(A)